

Delayed star-formation in high-redshift stream-fed galaxies

J. M. Gabor,^{1*} Frédéric Bournaud¹

¹CEA-Saclay, IRFU, SAp, F-91191 Gif-sur-Yvette, France

5 February 2018

ABSTRACT

We propose that star formation is delayed relative to the inflow rate in rapidly-accreting galaxies at very high redshift ($z > 2$) because of the energy conveyed by the accreting gas. Accreting gas streams provide fuel for star formation, but they stir the disk and increase turbulence above the usual levels compatible with gravitational instability, reducing the star formation efficiency in the available gas. After the specific inflow rate has sufficiently decreased – typically at $z < 3$ – galaxies settle in a self-regulated regime with efficient star formation. An analytic model shows that this interaction between infalling gas and young galaxies can significantly delay star formation and maintain high gas fractions ($>40\%$) down to $z \approx 2$, in contrast to other galaxy formation models. Idealized hydrodynamic simulations of infalling gas streams onto primordial galaxies confirm the efficient energetic coupling at $z > 2$, and suggest that this effect is largely under-resolved in existing cosmological simulations.

Key words: galaxies:evolution – galaxies:formation

1 INTRODUCTION

Star forming galaxies at redshift $z \approx 1 - 2$ have high gas fractions $\gtrsim 50\%$, probed by both their molecular gas and dust properties (Daddi et al. 2010; Magdis et al. 2012; Tacconi et al. 2013, but note criticism from Narayanan et al. 2012). Many galaxy evolution models under-predict gas fractions at high redshifts (Dutton et al. 2010; Davé et al. 2012), and cosmological simulations find gas fractions as low as 10% at $z \approx 1 - 2$ for stellar masses in the $10^{10} - 10^{11} M_{\odot}$ range (e.g. Ceverino et al. 2010; Kereš et al. 2012, but higher in some cases, e.g. Genel et al. 2012b). This likely results from a too-rapid consumption of gas reservoirs at $z > 2$, where observations suggest that the efficiency of star formation is more moderate (in proportions that remain contentious; Daddi et al. 2007; González et al. 2010; Elbaz et al. 2011; Bouwens et al. 2012; Reddy et al. 2012; Stark et al. 2013). The need to delay star formation in the $z > 2$ progenitors of star-forming galaxies, summarized by Bouché et al. (2010) and Weinmann et al. (2012), may (Henriques et al. 2013) or may not be solved by stellar feedback – recently simulated galaxies with stronger feedback still become star-dominated within their effective radii by $z \approx 3$, with excessive specific star formation rates at earlier epochs (Ceverino et al. 2013). Feedback from active galactic nuclei tends to exacerbate the problem by lowering gas fractions (Dubois et al. 2012a) if it has a substantial effect at all (cf. Gabor & Bournaud 2013). Low metallicity could play a role by hindering cooling (Krumholz & Dekel 2012). Here we examine another possibility to maintain high gas fractions: infalling gas streams could themselves delay star-formation.

Cosmological simulations indicate that galaxies are predominantly fed by relatively diffuse gas flowing along dark matter fil-

aments, rather than mergers (e.g. Kereš et al. 2005; Ocvirk et al. 2008; Brooks et al. 2009). If the kinetic energy from the infalling gas couples with the galactic disk, this may increase the turbulent velocity dispersion at early times (Elmegreen & Burkert 2010; Genel et al. 2012a), until grown-up galaxies at lower redshift manage to self-regulate their gas turbulence. We propose that this boosted velocity dispersion will tend to increase the physical size of the galaxy gas distribution, lowering the gas density and star formation efficiency. As we will show, the overall SF efficiency can be reduced by factors of about three at $z \geq 3$, making it possible to maintain high gas fractions of 40-50% down to $z \approx 2 - 3$. We study this process with an analytic model (§2) that combines the “bath tub” approach for galaxy evolution (Bouché et al. 2010; Davé et al. 2012; Lilly et al. 2013) with analytic descriptions of star formation in turbulent gas (Elmegreen 2002; Krumholz & Tan 2007) and accounts for the external energy supply. We also simulate the hydrodynamic interaction of galaxies with infalling gas streams (§3) and confirm that rapid gas infall feeds only reduced and delayed star formation in $z \approx 3 - 6$ conditions.

2 ANALYTIC MODEL

We develop an analytic model for galaxy evolution that combines three main physical elements: an estimate of self-regulated vs. infall-driven gas turbulence, a star-formation rate linked to the gas density and velocity dispersion, and a standard “bath-tub”-like mass budget.

(i) *Self-regulated vs. infall-driven gas turbulence:* We use an approach similar to Elmegreen & Burkert (2010) to determine the gas velocity dispersion. Internal processes in galaxies that generate turbulence (e.g. gravitational instabilities, radial flows, star forma-

* Email:jared.gabor@cea.fr

tion feedback) all saturate about the limit for gravitational instability, which corresponds to a Toomre parameter $Q = 0.7$ for thick disks (Dekel et al. 2009). These processes, regardless of their respective individual contribution, stir the gas disk at a minimal level $\sigma_{\min} = Q\pi G\Sigma_{\text{gas}}/\Omega\sqrt{2}$ below which the gas velocity dispersion cannot drop (in a steady state). Σ_{gas} is the gas surface density, and $\Omega = v_{\text{rot}}/r$ is the orbital frequency of the disk.

The next question is whether external gas infall *alone* can stir the disk above this internally-determined level. Because internal processes *saturate* at σ_{\min} , a contribution from external sources lower than σ_{\min} will not add turbulence – it will only decrease the relative contribution of internal sources in the σ_{\min} . External infall at a mass rate \dot{M}_{inflow} injects kinetic energy at a rate $\dot{E}_{\text{turb, infall}} = A_{\text{infall}} 0.5 \dot{M}_{\text{inflow}} v_{\text{infall}}^2$, where $v_{\text{infall}} = \sqrt{2} v_{\text{halo}} = \sqrt{2} (10GM_{\text{h}}H(z))^{1/3}$, M_{h} is the halo mass, and $H(z)$ is the redshift-dependent Hubble parameter (Croton et al. 2006). A_{infall} specifies the coupling efficiency of infall energy to the turbulent energy of the disk. For simplicity we assume that $A_{\text{infall}} = (\text{disk surface area})/(\text{stream cross-sectional area})$, with a maximum value of 1. We address the disk radius and thus the disk area below. We assume the typical cosmic stream radius to be $f_{\text{stream}} = 0.1$ times the virial radius of the characteristic Press-Schechter halo (cf. Dekel & Birnboim 2006). This typically gives $A_{\text{infall}} = 1$ at $z \gtrsim 2$ for the galaxies we study here, which is supported by our simulations in §3. The other key behavior of this coupling is that it becomes weak around $z = 2$, as required to prevent low- z disks from being too thick (Genel et al. 2012a). We discuss the coupling further at the end of §3.1.

While inflows add turbulent energy, dissipation of that energy occurs over $f_{\text{diss}} \approx 3$ disk dynamical times (cf. Mac Low et al. 1998; Gammie 2001), so that $\dot{E}_{\text{turb, diss}} = E_{\text{turb}}/\tau_{\text{diss}} = E_{\text{turb}}v_{\text{rot}}/(f_{\text{diss}}R_{\text{gal}})$, where v_{rot} is the galaxy rotation velocity, and R_{gal} is the radius. With the equations we track the turbulent energy in the gas, E_{turb} , and the velocity dispersion achievable from infall $\sigma_{\text{infall}} = \sqrt{2/3} E_{\text{turb}}/M_{\text{gas}}$. Because of the previously mentioned saturation effects, we assume that the gas settles at a velocity dispersion equal to $\max(\sigma_{\min}, \sigma_{\text{infall}})$.

(ii) **The star formation rate** is determined based not just on the gas density, but also on its velocity dispersion. We assume the gas takes on a log-normal density probability distribution function (PDF) typical of supersonic turbulence (e.g. Padoan et al. 1997), independent of the main source of turbulence. The peak of the log-normal is determined from the average gas density of the galaxy (see below) and the width of the PDF is $(\ln(1 + 0.75(\sigma/c_s)^2))^{1/2}$, where the sound speed c_s is assumed to be $\approx 10 \text{ km s}^{-1}$ for the star-forming gas (Padoan et al. 1997). We assume that gas at number densities above 100 cm^{-3} forms stars at a volumetric rate of $\dot{\rho}_* = \epsilon_* \rho/t_{\text{ff}} = \epsilon_* (32G\rho^3/(3\pi))^{1/2}$, where t_{ff} is the free-fall time and $\epsilon_* = 0.01$ is the local star-formation efficiency per free-fall time (cf. Krumholz et al. 2012). Numerical integration over the density PDF and galaxy volume gives the total SFR of the galaxy.

Determining the average gas density requires an estimate of the galaxy geometry. The disk radius depends on the galaxy's angular momentum, which is highly uncertain for high- z galaxies. For simplicity and consistency with previous work, we follow Krumholz & Dekel (2012) to obtain the standard, undisturbed disk scale radius of $R_{\text{scale}} = 0.5\lambda R_v$, where λ is the halo spin parameter and R_v is the halo virial radius. We use $\lambda = 0.07$ as a typical value (Dutton et al. 2011). This radius is increased when infalling gas increases the velocity dispersion and scatters gas to larger radii. We can estimate this effect by taking $v_{\text{rotation}}^2 \approx v_{\text{circ}}^2 - 3\sigma^2$ for the rotational specific energy, then assuming an-

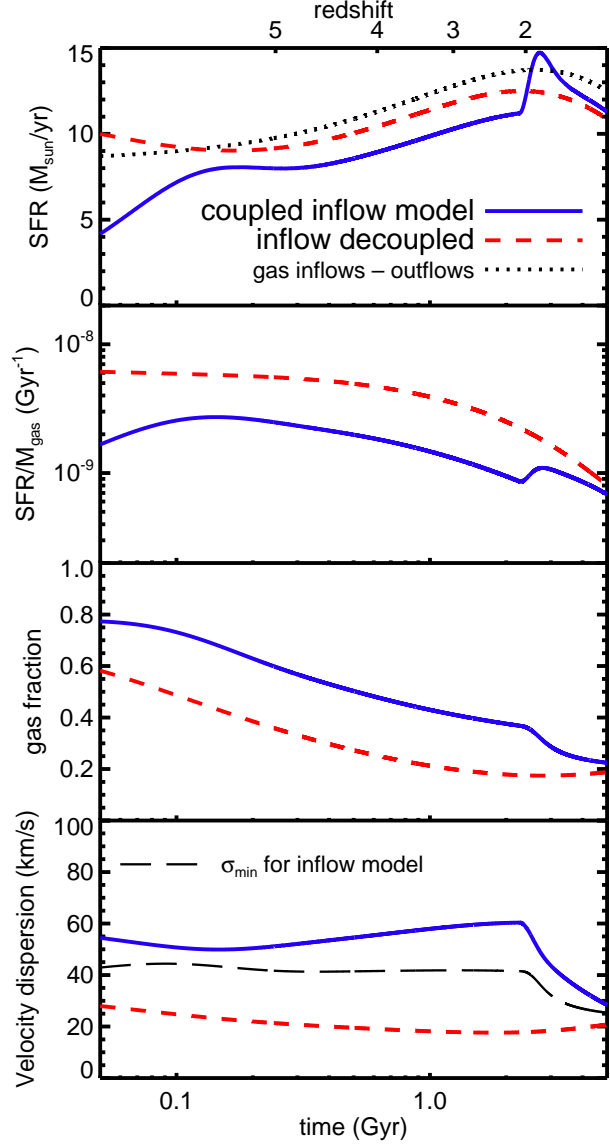


Figure 1. In our simple cosmological inflow model (solid blue lines), accreting gas suppresses star-formation, allowing a substantial gas reservoir to remain in place to $z < 2$. We compare this fiducial model with an otherwise identical model where infalling cold streams have no effect on the galaxy (other than to provide fuel for SF; dashed red lines). **Top:** The SFR is suppressed by $\sim 25\%$ due to infalling gas at high redshifts. We also show net gas inflows to the galaxy for comparison (dotted line). **Second panel:** Global galaxy SF efficiency, $\text{SFR}/M_{\text{gas}}$, is reduced by a factor of ~ 3 due to inflows. **Third panel:** Gas fraction. By suppressing the SFR, infalling cold streams allow the gas fraction to remain high. **Bottom:** Velocity dispersion. For the coupled-inflows model, we also show σ_{\min} (long-dashed line). Infalling cold streams increase the velocity dispersion by up to $\sim 50\%$ compared to σ_{\min} , and a factor of 3 above the control simulation (which has a lower gas fraction).

gular momentum is approximately conserved with $R_{\text{scale}}v_{\text{circ}} \approx R_{\text{disturbed}}v_{\text{rotation}}$. Here v_{circ} is the circular velocity and v_{rotation} is the actual rotational velocity. The disk scale radius becomes $R_{\text{disturbed}} \approx R_{\text{scale}}(1.0 - 3\sigma^2/v_{\text{circ}}^2)^{-1/2}$. For simplicity, we multiply this scale radius by 1.7 to obtain the total disk radius, as appropriate for exponential disks. The scale height of the gas disk is given by $H = \sigma^2/(\pi G\Sigma_{\text{s+g}})$, where $\Sigma_{\text{s+g}}$ is the total mass sur-

face density of stars and gas in the disk. Thus, when inflowing gas streams increase σ , both the radius and scale height increase. The average gas density decreases because the rapidly infalling gas does not immediately settle into a thin, self-gravitating disk.

(iii) **“Bath tub”-like mass budget:** Cosmological inflow acts as a gas source, while star formation and galactic winds act as sinks. We take the cosmological mass inflow rate of gas into a dark matter halo of mass M_h at redshift z to be $\dot{M}_{\text{inflow}} = 6.6 f_b (M_h/10^{12})^{1.15} (1+z)^{2.25}$ (Dekel et al. 2009). We assume that the cosmological fraction of baryons $f_b = 16.5$ per cent accompanies the dark matter into the halo, and for simplicity we assume the baryons all enter as gas via cold streams (rather than mergers). Although recent simulations raise doubt that cold streams can penetrate the halo (Nelson et al. 2013), they are likely the dominant mode of galaxy fueling in low mass halos at high- z . Star-formation (as described above) removes gas from the galaxy’s reservoir, and we assume that young stars drive galactic winds that eject gas from the galaxy at a rate equal to the SFR.

Using these equations to track the turbulent energy, star-formation, and gas reservoir, we evolve a model galaxy over cosmic time with a simple numerical integration scheme. To make the discussion concrete, we focus on a Milky Way progenitor galaxy with an initial halo mass of $5 \times 10^{10} M_\odot$ at $z = 6$ and a final ($z = 0$) halo mass of $1.7 \times 10^{12} M_\odot$. The galaxy has an initial baryonic mass of $2.5 \times 10^9 M_\odot$, an initial gas fraction of 75 per cent, and an initial velocity dispersion of 50 km s^{-1} , but the galaxy rapidly evolves towards an equilibrium independent of these choices.

2.1 Results of the inflow model

Figure 1 compares the results of our fiducial coupled-inflow model with a control model, in which inflow is decoupled from the disk. In the decoupled model, the galaxy has the same mass inflow rate, but we neglect any energy coupling between inflows and the disk.

At $z > 2$ in our infall model (solid blue lines), inflows are strongly coupled to the galactic disk. They deposit turbulent energy into the disk, causing a boost in the velocity dispersion (bottom panel). The boosted velocity dispersion slightly lowers the average gas density of the galaxy, thus lowering the global SF efficiency and SFR. Because the SF efficiency is suppressed, gas is allowed to accumulate in the galaxy, leading to a sustained high gas fraction (higher by a factor of ~ 2). The specific SFR remains almost unchanged compared to the control model because both the SFR and stellar mass are suppressed by infall.

At $z = 2$ the coupling between the infalling cold streams and galaxy disk becomes less efficient (with an abruptness owing to our simple assumptions about A_{infall}). This occurs when the typical filament size equals the size of the galaxy disk. When the coupling weakens, the turbulent energy in the disk decays, causing the velocity dispersion to decline (bottom panel near $z = 2$). This leads to an increase in gas density that causes a brief spike in the SFR (top panel). The gas fraction begins to decrease and eventually the SFR does as well, and all quantities converge toward the “decoupled inflow” model at low redshifts. The galaxy converges towards its normal state as a self-regulated, star-forming disk.

In summary, the main effect of infalling gas is to increase the velocity dispersion, “puff up” the galaxy disk, lower the SFR and SF efficiency, and increase the gas fraction. These effects persist as long as the coupling between infalling gas and the galaxy disk is strong (as we have assumed). When the coupling becomes weak (at $z \approx 2$ in our model), the galaxy converges towards the solution where infalling gas is decoupled from the disk.

3 SIMULATIONS

To test our model, we simulate the accretion of cold gas flows by young galaxies with the Adaptive Mesh Refinement (AMR) code RAMSES (Teyssier 2002). A key difference with existing idealized and cosmological simulations is that we ensure relatively high resolution in low-density gas, at the expense of the maximal resolution in the densest regions. We start with a coarse grid of resolution 1.0 kpc, and refine each cell into eight smaller cells when its gas mass exceeds $200 M_\odot$ and/or it contains more than 240 particles (of stars and/or dark matter). The maximal resolution of 32 pc is ensured as soon as the gas number density exceeds 0.2 cm^{-3} (with 64 pc resolution at 0.025 cm^{-3}). We allow cooling down to 10^4 K and enforce a pressure floor to keep the Jeans length resolved by at least four cells.

Old stars, new stars and dark matter are modeled with particles of 2×10^3 , 800, and $8 \times 10^3 M_\odot$, respectively. Star-formation occurs in gas denser than 1 cm^{-3} , with an efficiency of 0.01 per local gravitational free-fall time (cf. Zuckerman & Evans 1974). The low density threshold ensures that variations in the SFR are not caused by artefacts near the highest resolvable densities, although in practice most of the SFR is obtained from gas at and above 100 cm^{-3} . We include stellar feedback – photoionization and radiation pressure, using the Renaud et al. (2013) model with a trapping parameter $\kappa = 5$, and supernovae feedback: ten Myrs after its birth, a star particle dumps thermal energy in the nearest gas cell, at a rate of 10^{51} ergs for each $10 M_\odot$ of progenitor mass. We account for non-thermal processes in supernova remnants by decreasing the gas cooling rate in the affected cells, as proposed by Teyssier et al. (2013). This can also be seen as a way to prevent over-cooling of the thermal phases in supernovae remnants (cf. Stinson et al. 2006).

We use two galaxy models, roughly representative of progenitors of Milky Way-mass galaxies at redshifts $z \approx 5$ and $z \approx 1 - 2$. They start with a stellar mass of $1.3 \times 10^9 M_\odot$ for $z \approx 5$ (respectively $8.0 \times 10^{10} M_\odot$ for $z \approx 1 - 2$) and a gas fraction of 75 per cent (resp. 50 per cent). The disk scale-length is 1.8 kpc (resp. 4 kpc) and a bulge of radius 240 pc (resp. 500 pc) contains 15 per cent of the stellar mass. Dark matter halos with NFW profiles are used with concentration parameters set to 7.0. A hot ($> 10^6 \text{ K}$) atmosphere is included with an homogeneous density (a few $\times 10^{-5} \text{ cm}^{-3}$) such that the mass comprised in the dark halo virial radius is 37% of the disk mass.

Each galaxy is modeled with and without accreting cosmological streams. The inflow rate is $15 M_\odot \text{ yr}^{-1}$ for the $z \approx 5$ case and $80 M_\odot \text{ yr}^{-1}$ for the $z \approx 1 - 2$ one – for the lower-mass, higher-redshift progenitor, this corresponds to a twelve times higher specific inflow rate at $z \approx 5$, as expected from theory (cf. §2). The inflowing gas is introduced in three streams. The streams originate at a distance from the galaxy center equal to 1.2 times the virial radius of the dark matter halo. They have a circular cross-section with an azimuthal profile as follows: a central density set by the required inflow rate, an exponential decay with a scale-length equal to the galaxy disk radius, and a truncation at 2.5 times this scale length. In the disk frame, the streams are set to cross the virial radius at latitudes of (+35, -45 and +65) degrees, respectively, and longitudes of (-90, +90 and +180) degrees, respectively. They contain respectively 45, 35 and 20 percent of the mass inflow rate, have impact parameters of 1.5, 2.0 and 1.5 disk scale lengths with prograde orientations except for the third and weakest one. This configuration, while arbitrary, is consistent with cosmological simulations (cf. Danovich et al. 2012), and so is the gas density along the flow

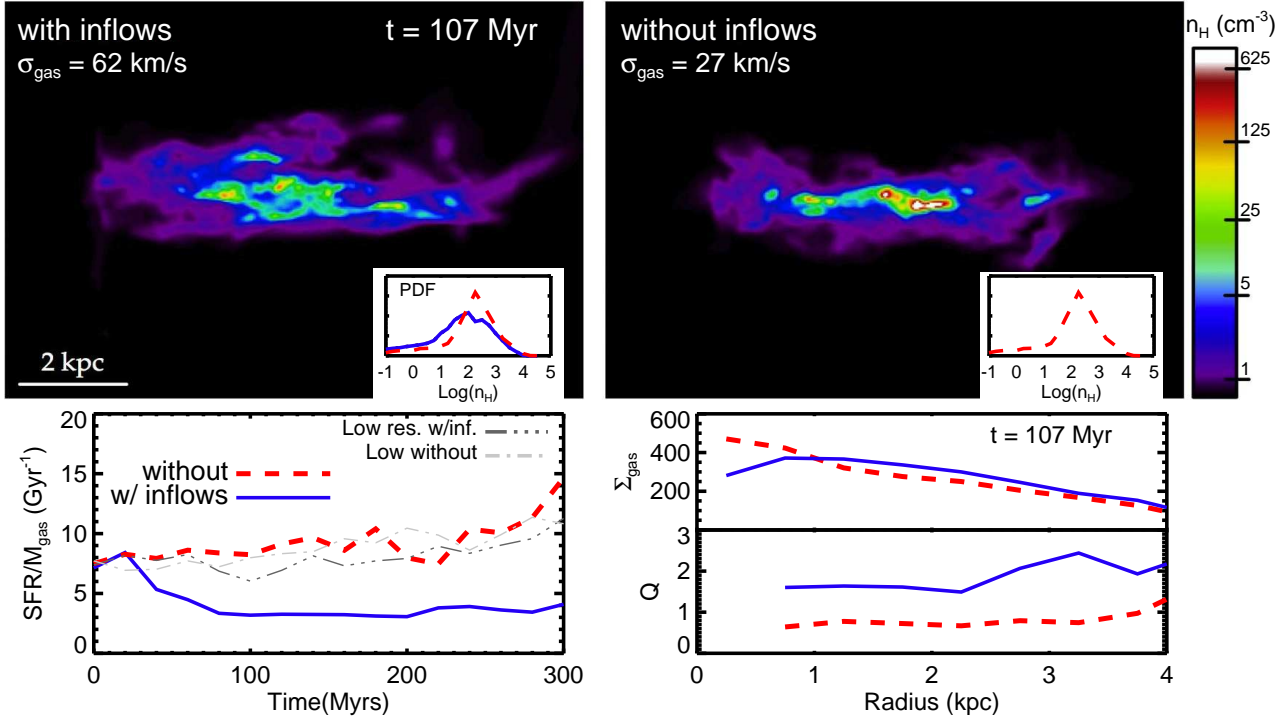


Figure 2. Top: Gas density images of simulations of a $z \sim 5$ isolated galaxy with (left) and without (right) cold inflows, at a time $t = 107$ Myr after the cold streams meet the disk. Cold inflows increase the gas velocity dispersion and scale height of the galaxy. Inflows also lead to a (normalised) density PDF (inset panels) with less gas at high, star-forming densities (i.e. $> 10^2 \text{ cm}^{-3}$). **Bottom left:** The SF efficiency ($\text{SFR}/M_{\text{gas}}$) is 2–3 times lower with inflows (blue solid lines) than without (red dashed). We also show results for low-resolution simulations with and without inflows (gray dot-dashed lines) – without sufficient resolution, the SFE is unaffected by inflows. **Bottom right:** Radial profiles of gas surface density Σ_{gas} (in $M_{\odot} \text{ pc}^{-2}$) and Toomre Q parameter. Inflows lower the gas surface density within the central regions, and increase the stability to $Q > 1$ across the disk.

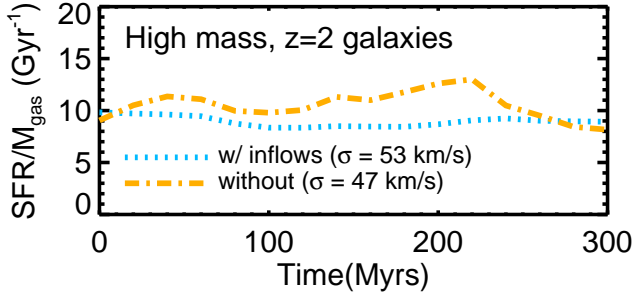


Figure 3. SF efficiencies vs. time for our two massive $z = 2$ galaxy simulations. In this case, the effect of cold inflows is weak, typically changing the SF efficiency by ~ 20 per cent or less.

axis ($0.01 - 0.05 \text{ cm}^{-3}$, $\sim 10^3$ times lower than the average initial density in the galaxy).

3.1 Simulation results

We simulate each galaxy for ≈ 2 rotation periods (300+ Myr). Figure 2 shows edge-on gas maps of the two low-mass $z \sim 5$ galaxies at $t = 107$ Myrs. The cold inflows puff up the disk, leaving the galaxy with fewer regions at the highest densities. Inflows increase the effective scale height from 325 pc to 612 pc, and the half-mass radius from 2.12 kpc to 2.86 kpc. We measure mass-weighted gas velocity dispersions and star-formation rates within 5 kpc of the galaxy center, along with radial profiles of gas surface density and an estimate

of the Toomre Q parameter (assuming the gas and stellar velocity dispersions are equal). The velocity dispersion in the inflows simulation is higher by a factor of ~ 2 , leading to a thicker disk and a SF efficiency lower by a factor of $\sim 2 - 3$. The figure also shows the (volume) density PDFs of the two simulations, illustrating that cold inflows can reduce the amount of gas at high, star-forming densities above 100 cm^{-3} . The lower right panels show that the central gas surface density, Σ_{gas} , is actually decreased due to inflows. Rather than merely adding gas to the galaxy, the inflows contribute energy that stabilises the disk at all radii, as indicated by the boosted Toomre Q parameter.

Thus abundant, filamentary cold gas inflows can disturb small galaxies at $z \sim 5$, boosting the velocity dispersion and effectively lowering the SFR. For more massive galaxies at lower redshifts, the cold streams do not affect the gas disk as strongly, as demonstrated by our $z \sim 2$ simulations. In these simulations the velocity dispersion is barely changed (53 km s^{-1} with inflows versus 47 km s^{-1} without), and the SF efficiency remains within ~ 20 per cent, as shown in Figure 3. This agrees qualitatively with the ‘high-redshift’ simulations of Hopkins et al. (2013), which are broadly representative of massive $z \sim 2$ galaxies. We speculate that the $\sim 10\times$ higher specific inflow rate ($\dot{M}_{\text{inflow}}/M_{\text{gas}}$) in our low-mass $z \sim 5$ galaxies leads to a stronger coupling between infalling gas and the disk. Cosmological simulations – even zoom-ins – generally lack the resolution in the low-density circumgalactic gas to model this effect accurately (although they do show a messy, rapidly varying connection region between filaments and the galaxy, e.g. Danovich et al. 2012; Dubois et al. 2012b).

These simulations imply that energy from infalling streams

can, at least under some circumstances, couple strongly to the galactic disk. In our analytic model (§2) we posit that the coupling (A_{infall}) is strong at $z > 2$ and then weakens as the streams become larger than the galaxy. Our simulations, though limited in the scope of parameter space, suggest instead a dependence of the coupling on halo mass or specific accretion rate. This dependence also leads to reduced SF efficiency at high- z followed by a transition to normal efficiency at lower z . Another possibility is that cold streams are disrupted before they fully penetrate the halo (Nelson et al. 2013) – while such disruption precludes interaction with the disk, it could effectively delay star-formation by prolonging the time spent in the circum-galactic reservoir. In our simulations the streams penetrate an idealised hot atmosphere without disruption, but cosmological simulations with high resolution in a more realistic circum-galactic gas distribution may be needed to confirm this result. Although some physical details remain in question, our model and simulations support a scenario where infalling cold streams delay star formation in low-mass galaxies at high- z , but have little effect on their more massive descendants at $z \lesssim 2$.

4 CONCLUSION

Our simple model of cold gas inflows into high-redshift galaxies shows that if the coupling between inflows and the gas disk is strong, then inflows can lower the star-formation efficiencies by factors of 3 and keep gas fractions above 40 per cent until $z < 2$. While previous models suggest the coupling between inflows and the disk is fairly weak (e.g. Klessen & Hennebelle 2010; Hopkins et al. 2013), our simulations with inflows show that this coupling can be strong if enough gas is inflowing. When the coupling is strong, cold flows don't settle into a self-regulated disk, but rather stir up the disk and suppress star-formation. Our work implies that in the high- z Universe where galaxies are small and inflow rates are large, the energetic injection of cold inflows has an important impact on galaxy evolution.

ACKNOWLEDGEMENTS

We thank Romain Teyssier for making RAMSES publicly available; the referee for prompt and thoughtful comments; and Daniel Ceverino, Avishai Dekel, and Florent Renaud for useful discussions. We acknowledge support from the EC through grants ERC-StG-257720 and the CosmoComp ITN. Simulations were performed at TGCC and as part of a GENCI project (grants 2011-042192 and 2012-042192).

REFERENCES

- Bouché N. et al., 2010, *ApJ*, 718, 1001
 Bouwens R. J. et al., 2012, *ApJ*, 754, 83
 Brooks A. M., Governato F., Quinn T., Brook C. B., Wadsley J., 2009, *ApJ*, 694, 396
 Ceverino D., Dekel A., Bouchard F., 2010, *MNRAS*, 404, 2151
 Ceverino D., Klypin A., Klimek E., Trujillo-Gomez S., Churchill C. W., Primack J., Dekel A., 2013, *ArXiv e-prints*
 Croton D. J. et al., 2006, *MNRAS*, 365, 11
 Daddi E. et al., 2010, *ApJ*, 713, 686
 Daddi E. et al., 2007, *ApJ*, 670, 156
 Danovich M., Dekel A., Hahn O., Teyssier R., 2012, *MNRAS*, 422, 1732
 Davé R., Finlator K., Oppenheimer B. D., 2012, *MNRAS*, 421, 98
 Dekel A., Birnboim Y., 2006, *MNRAS*, 368, 2
 Dekel A., Sari R., Ceverino D., 2009, *ApJ*, 703, 785
 Dubois Y., Devriendt J., Slyz A., Teyssier R., 2012a, *MNRAS*, 420, 2662
 Dubois Y., Pichon C., Haehnelt M., Kimm T., Slyz A., Devriendt J., Pogosyan D., 2012b, *MNRAS*, 423, 3616
 Dutton A. A., van den Bosch F. C., Dekel A., 2010, *MNRAS*, 405, 1690
 Dutton A. A. et al., 2011, *MNRAS*, 410, 1660
 Elbaz D. et al., 2011, *A&A*, 533, A119
 Elmegreen B. G., 2002, *ApJ*, 577, 206
 Elmegreen B. G., Burkert A., 2010, *ApJ*, 712, 294
 Gabor J. M., Bournaud F., 2013, *MNRAS*, 434, 606
 Gammie C. F., 2001, *ApJ*, 553, 174
 Genel S., Dekel A., Cacciato M., 2012a, *MNRAS*, 425, 788
 Genel S., Naab T., Genzel R., Förster Schreiber N. M., Sternberg A., Oser L., Johansson P. H., Davé R., Oppenheimer B. D., Burkert A., 2012b, *ApJ*, 745, 11
 González V., Labbé I., Bouwens R. J., Illingworth G., Franx M., Kriek M., Brammer G. B., 2010, *ApJ*, 713, 115
 Henriques B. M. B., White S. D. M., Thomas P. A., Angulo R. E., Guo Q., Lemson G., Springel V., 2013, *MNRAS*, 431, 3373
 Hopkins P. F., Kereš D., Murray N., 2013, *MNRAS*, 432, 2639
 Kereš D., Katz N., Weinberg D. H., Davé R., 2005, *MNRAS*, 363, 2
 Kereš D., Vogelsberger M., Sijacki D., Springel V., Hernquist L., 2012, *MNRAS*, 425, 2027
 Klessen R. S., Hennebelle P., 2010, *A&A*, 520, A17
 Krumholz M. R., Dekel A., 2012, *ApJ*, 753, 16
 Krumholz M. R., Dekel A., McKee C. F., 2012, *ApJ*, 745, 69
 Krumholz M. R., Tan J. C., 2007, *ApJ*, 654, 304
 Lilly S. J., Carollo C. M., Pipino A., Renzini A., Peng Y., 2013, *ApJ*, 772, 119
 Mac Low M.-M., Klessen R. S., Burkert A., Smith M. D., 1998, *Physical Review Letters*, 80, 2754
 Magdis G. E. et al., 2012, *ApJ*, 760, 6
 Narayanan D., Bothwell M., Davé R., 2012, *MNRAS*, 426, 1178
 Nelson D., Vogelsberger M., Genel S., Sijacki D., Kereš D., Springel V., Hernquist L., 2013, *MNRAS*, 429, 3353
 Ocvirk P., Pichon C., Teyssier R., 2008, *MNRAS*, 390, 1326
 Padoan P., Jones B. J. T., Nordlund A. P., 1997, *ApJ*, 474, 730
 Reddy N. A., Pettini M., Steidel C. C., Shapley A. E., Erb D. K., Law D. R., 2012, *ApJ*, 754, 25
 Renaud F. et al., 2013, *ArXiv e-prints*
 Stark D. P., Schenker M. A., Ellis R., Robertson B., McLure R., Dunlop J., 2013, *ApJ*, 763, 129
 Stinson G., Seth A., Katz N., Wadsley J., Governato F., Quinn T., 2006, *MNRAS*, 373, 1074
 Tacconi L. J. et al., 2013, *ApJ*, 768, 74
 Teyssier R., 2002, *A&A*, 385, 337
 Teyssier R., Pontzen A., Dubois Y., Read J. I., 2013, *MNRAS*, 429, 3068
 Weinmann S. M., Pasquali A., Oppenheimer B. D., Finlator K., Mendel J. T., Crain R. A., Macci'o A. V., 2012, *MNRAS*, 426, 2797
 Zuckerman B., Evans II N. J., 1974, *ApJ*, 192, L149